Common force field for graphite and polycyclic aromatic hydrocarbons

C. Mapelli, C. Castiglioni, and G. Zerbi
Dipartimento di Chimica Industriale e Ingegneria Chimica, Politecnico di Milano, Piazza Leonardo Da Vinci 32, 20133 Milano, Italy

K. Müllen
Max-Plank-Institut für Polymerforschung, Ackermannweg 10, D-55128 Mainz, Germany
(Received 11 June 1999; revised manuscript received 28 July 1999)

A valence force field based on Hückel's theory has been developed, which allows us to establish a close correlation between phonons of graphite and the normal modes of small polycyclic aromatic hydrocarbons (such as coronene and hexabenzocoronene). The results show that in these systems two kinds of motions dominate the Raman spectrum: the Я mode and the ''breathing'' ☋ mode. These modes are the equivalent, in a finite domain, of the E_{2g} phonon of graphite at the Γ point and the A' phonon at the K point of the first Brillouin zone. This study provides a useful basis for the understanding of the Raman spectra of any material containing sp^2 carbon domains. [S0163-1829(99)01542-8]

I. INTRODUCTION

Carbon-based materials, ranging from highly oriented pyrolitic graphite to polycrystalline graphite and from Diamond-like-carbon to carbon nanotubes, have been extensively studied over the past two decades because of their numerous and relevant technological applications.[1] The macroscopic properties of these materials are strongly modified by the structure of the compound on atomic scale. The relative amount of sp^2 and sp^3 carbon atoms, the dimensions of the aromatic domains in graphite, and the occurrence of defects are only a few of the ''parameters'' that vary in function of the method of preparation. It is then important to develop tools for an accurate structural characterization of these materials: the aim of these kinds of work is to establish structure/property relationships, which may become useful in obtaining improved materials with optimized properties for specific applications.

Raman spectroscopy is a powerful means of structural diagnosis: Raman spectra of a wide variety of carbon-based materials are reported in a very abundant literature and have often been used with success for sample characterization.[1] Problems arise, however, when spectral features are not used in a merely correlative way but they must be related to a precise structural model.

One of the most intriguing problems, which is still debated, is the correct assignment of the so-called *D* Raman line of graphite, that is always observed in the spectra of graphitic materials with a certain degree of disorder. The shift of the *D* line with the exciting laser frequency was observed many years ago;[2] very recently, systematic studies have related the shift of the *D* line to the occurrence of resonance enhancement effects.[3,4] At the same time, a close correlation between the Raman patterns of disordered graphite and of polycyclic aromatic hydrocarbons (PAHs) has been observed by the authors.[5] A systematic and comparative study of PAH's and graphite spectra would be useful in order to clarify the origin of the *D* line and its resonance behavior. The first step in this research is to build a common basis for the analysis of Raman spectra of graphite and of the related molecular models.

In this paper we describe the vibrational dynamics of PAH's and graphite aiming to develop a valence force field that could be used for any kind of carbon sp^2 system, regardless of size and shape, and for graphite too. Such a field would allow us to have a common ground in the interpretation of the vibrational spectra of these materials. This is done in this work taking a force field proposed by Ohno,[6] known as MO/8 field, which has been shown to be suitable for PAH's of different size and shape[6] and generalizing it to the case of an infinite two-dimensional layer of graphite. On the basis of this force field the relevant spectral features of PAH molecules can be correlated, on analytic grounds, to those observed in graphite samples.

II. FORCE FIELD: METHOD

The MO/8 field has been shown to be suitable for the analysis of the in-plane vibrations of some condensed hydrocarbons.[6] It takes into account the following force constants:

diagonal CC stretching:

$$F_{ii}=f_1+f_2(p_i-p_0)+f_3(\Pi_{ii}-\Pi_0), \tag{1}$$

off-diagonal CC stretching interactions:

$$F_{ij}=f_3\Pi_{ij} \quad (i\neq j), \tag{2}$$

diagonal CH stretching: f_4,

diagonal CCC bending: f_5,

diagonal CCH bending: f_6,

off-diagonal CC-CCC interaction: f_7,

off-diagonal CC-CCH interaction: f_8.

Equations (1) and (2) have been derived according to Hückel's theory.[7,8] p_i and Π_{ij} are, respectively, the bond order of the ith bond and the bond-bond polarizability of bonds i and

j of the molecule; p_0 and Π_0 are the bond order and self-bond polarizability for benzene.

In a finite molecule the total mobile bond order of a pair of bonded atoms t and s, as defined by Coulson and Longuet-Higgens,[9] is

$$P_{ts}=\sum_{l=1}^{m} n_l c_{lt} c_{ls}, \tag{3}$$

where the summation is over all the occupied orbitals, n_l is the number of electrons in the lth orbital, and c_{lt} and c_{ls} are Hückel's coefficients for the lth orbital on atoms t and s of the molecule. The bond-bond polarizability between bonds ts and vu can be written as

$$\Pi_{ts,vu}=2\sum_{l=1}^{m}\sum_{k=m+1}^{N}\frac{(c_{tl}c_{sk}+c_{sl}c_{tk})(c_{vl}c_{uk}+c_{ul}c_{vk})}{\varepsilon_l-\varepsilon_k}. \tag{4}$$

Ohno's force field can be generalized for a layer of graphite, provided that expressions (3) and (4) are extended to a periodic and infinite system.[10] A layer of graphite can be considered as a two-dimensional crystal that can be described using a hexagonal lattice with two atoms per cell [Fig. 1(a)]. Each atom in the lattice can be identified using three indices: n_1 and n_2, which identify the cell in the lattice, and a number (1 or 2), which identifies the atom inside the cell. A molecular orbital of graphite can be written, according to the LCAO linear combination of atomic orbitals theory, as a linear combination of atomic orbitals

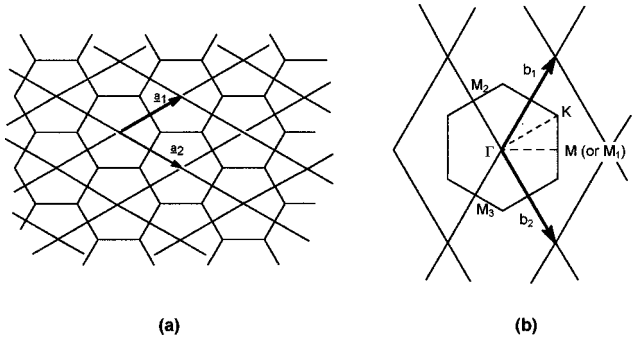

FIG. 1. (a) Lattice of graphite $\mathbf{a}_1$ and $\mathbf{a}_2$ are the fundamental vectors of the lattice. (b) Reciprocal lattice of graphite and first Brillouin zone.

$$\psi=\sum_{n_1}\sum_{n_2}(c_{n_1n_21}\phi_{n_1n_21}+c_{n_1n_22}\phi_{n_1n_22}). \tag{5}$$

$\phi_{n_1n_21}$ and $\phi_{n_1n_22}$ represent the p_z atomic orbital on carbon atoms $(n_1,n_2,1)$ and $(n_1,n_2,2)$; in fact only π molecular orbitals are considered in Hückel's theory. The coefficients of the combination can be written using Bloch's theorem. Neglecting the overlap between atomic orbitals (a.o.) and assuming each a.o. to be normalized, the expectation value for the energy of an electron in the molecular orbital is

$$y=\frac{\{(c_1^*c_1+c_2^*c_2)\alpha+c_1^*c_2\lfloor\beta(1+e^{-i\theta_1}+e^{-i\theta_2})\rfloor+c_2^*c_1\lfloor\beta(1+e^{i\theta_1}+e^{i\theta_2})\rfloor\}}{(c_1^*c_1+c_2^*c_2)},$$

where α is the Coulomb integral for a carbon atom, β is the resonance integral for any pair of *bonded* atoms, and θ_1 and θ_2 are the components of a $\mathbf{k}$ vector in the reciprocal space ($\mathbf{k}=\theta_1\mathbf{b}_1+\theta_2\mathbf{b}_2$). The values of α and β are fixed quantities, characteristic of the system. We can measure[11] the energy with reference to α and in units of β, i.e., we set $\alpha=0$ and $\beta=-1$.

Using the variation method one obtains the following expressions for the electronic energy in valence (ε_V) and conduction (ε_C) bands:

$$\varepsilon_V=-\sqrt{\{3+2\lfloor\cos(\theta_1-\theta_2)+\cos\theta_1+\cos\theta_2\rfloor\}}, \tag{6}$$

$$\varepsilon_C=\sqrt{\{3+2\lfloor\cos(\theta_1-\theta_2)+\cos\theta_1+\cos\theta_2\rfloor\}}. \tag{7}$$

Hereafter the subscripts V and C will be used to denote, respectively, the valence and the conduction bands. Imposing the normalization condition on a cell ($c_1^*c_1+c_2^*c_2=1$) one obtains the following values for Hückel's coefficients of cell (0, 0):

Valence band:

$$c_{V,1}=\frac{1}{\sqrt{2}}e^{-i\eta/2}, \tag{8a}$$

$$c_{V,2}=\frac{1}{\sqrt{2}}e^{i\eta/2}.$$

Conduction band:

$$c_{C,1}=-\frac{1}{\sqrt{2}}e^{-i\eta/2}, \tag{8b}$$

$$c_{C,2}=\frac{1}{\sqrt{2}}e^{i\eta/2},$$

where

$$e^{-i\eta}=\frac{(1+e^{-i\theta_1}+e^{-i\theta_2})}{\sqrt{(1+e^{i\theta_1}+e^{i\theta_2})(1+e^{-i\theta_1}+e^{-i\theta_2})}}. \tag{9}$$

Expressions (3) and (4) must be rewritten considering that Hückel's coefficients are now complex and that the summation over all the orbitals is infinite.

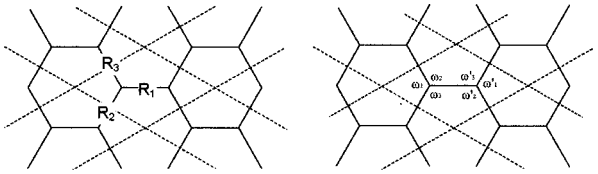

FIG. 2. Internal coordinates in the cell (0,0) of graphite.

The invariance of bond order under exchange of two atoms is taken into account by writing

$$p_{ts}=\sum_{i=1}^{m}(c_{it}^{*}c_{is}+c_{is}^{*}c_{it}). \tag{10}$$

The summation can be substituted by integration over the first Brillouin zone:

$$p_{ts}=\frac{1}{(2\pi)^2}\int_{-\pi}^{\pi}\int_{-\pi}^{\pi}[c_{V,t}^{*}(\theta_1,\theta_2)c_{V,s}(\theta_1,\theta_2)+c_{V,t}(\theta_1,\theta_2)c_{V,s}^{*}(\theta_1,\theta_2)]d\theta_1 d\theta_2, \tag{11}$$

in which only the coefficients of the valence band appear since the summation in Eq. (10) was only over occupied orbitals. The factor $1/(2\pi)^2$ appears as a consequence of normalization, since θ_1 and θ_2 take values between $-\pi$ and π.

At equilibrium, because of the symmetry of the lattice, all bonds are equivalent; as a consequence the value of p_{ts} does not depend on the pair *ts* (provided that *t* and *s* are bonded atoms) and will be denoted hereafter simply as *p*.

Substituting the expression for the coefficients of cell (0, 0) in Eq. (11) yields

$$p=\frac{1}{(2\pi)^2}\int_{-\pi}^{\pi}\int_{-\pi}^{\pi}\frac{1+\cos\theta_1+\cos\theta_2}{\sqrt{3+2[\cos\theta_1+\cos\theta_2+\cos(\theta_1-\theta_2)]}}d\theta_1 d\theta_2. \tag{12}$$

The bond-bond polarizability must be rewritten so that it is invariant under exchange of two bonds:[12]

$$\Pi_{ts,vu}=\sum_{i=1}^{m}\sum_{j=m+1}^{N}\frac{(c_{iv}^{*}c_{ju}+c_{iu}^{*}c_{jv})(c_{it}^{*}c_{js}+c_{is}^{*}c_{jt})+\text{c.c.}}{\varepsilon_i-\varepsilon_j}. \tag{13}$$

We introduce the integration over the entire Brillouin zone and obtain

$$\Pi_{ts,vu}=\frac{1}{(2\pi)^4}\int_{-\pi}^{\pi}\int_{-\pi}^{\pi}\int_{-\pi}^{\pi}\int_{-\pi}^{\pi}\frac{[c_{V,v}^{*}(\theta)c_{C,u}(\theta')+c_{V,u}^{*}(\theta)c_{C,v}(\theta')][c_{V,t}^{*}(\theta)c_{C,s}(\theta')+c_{V,s}^{*}(\theta)c_{C,t}(\theta')]+\text{c.c.}}{\varepsilon_V-\varepsilon_C}\times d\theta_1 d\theta_2 d\theta_1' d\theta_2', \tag{14}$$

where θ identifies the pair (θ_1,θ_2) which runs over the valence orbitals and θ' identifies the pair (θ_1',θ_2') which runs over the conduction orbitals.

Let R_1, R_2, and R_3 be the three CC bonds associated with one cell (Fig. 2). Expression (14) can be further modified observing that the translational invariance allows us to consider only interactions where *ts* is bond R_1 of the cell (0, 0). If the first bond is fixed, there are only two kinds of polarizability: the one between $R_1(0,0)$ and all the bonds $R_1(n_1,n_2)$, which will be called $\Pi^{\mathrm{I}}(n_1,n_2)$, and the interaction between $R_1(0,0)$ and $R_2(n_1,n_2)$, which will be called $\Pi^{\mathrm{II}}(n_1,n_2)$. Because of symmetry, the interaction between $R_1(0,0)$ and $R_3(n_1,n_2)$ equals the interaction between $R_1(0,0)$ and $R_2(n_2,n_1)$.

We can thus write two kinds of polarizability for graphite:

$$\Pi^{\mathrm{I}}(n_1,n_2)=\frac{1}{(2\pi)^4}\int_{-\pi}^{\pi}\int_{-\pi}^{\pi}\int_{-\pi}^{\pi}\int_{-\pi}^{\pi}\frac{[1-\cos(\eta+\eta')]\cos\Delta\theta}{\varepsilon_v-\varepsilon_c}d\theta_1 d\theta_2 d\theta_1' d\theta_2',$$

$$\Pi^{\mathrm{II}}(n_1,n_2)=\frac{1}{2(2\pi)^4}\times\int_{-\pi}^{\pi}\int_{-\pi}^{\pi}\int_{-\pi}^{\pi}\int_{-\pi}^{\pi}\frac{[1-\cos(\eta+\eta')][\cos(\Delta\theta+\theta_1)+\cos(\Delta\theta-\theta_1')]+\sin(\eta+\eta')[\sin(\Delta\theta-\theta_1')-\sin(\Delta\theta+\theta_1)]}{\varepsilon_v-\varepsilon_c}\times d\theta_1 d\theta_2 d\theta_1' d\theta_2', \tag{15}$$

where

$$\cos(\eta+\eta')=\frac{(1+\cos\theta_1+\cos\theta_2)(1+\cos\theta_1'+\cos\theta_2')-(\sin\theta_1+\sin\theta_2)(\sin\theta_1'+\sin\theta_2')}{\varepsilon_v\varepsilon_c},$$

$$\sin(\eta+\eta')=\frac{(\sin\theta_1+\sin\theta_2)(1+\cos\theta_1'+\cos\theta_2')+(\sin\theta_1'+\sin\theta_2')(1+\cos\theta_1+\cos\theta_2)}{\varepsilon_v\varepsilon_c},$$

$$\varepsilon_v=\sqrt{3+2[\cos\theta_1+\cos\theta_2+\cos(\theta_1-\theta_2)]},\quad \varepsilon_c=\sqrt{3+2[\cos\theta_1'+\cos\theta_2'+\cos(\theta_1'-\theta_2')]},$$

and

$$\Delta\theta=n_1(\theta_1'-\theta_1)+n_2(\theta_2'-\theta_2).$$

III. DYNAMICS CALCULATION

A. Force field

We have assumed for graphite a structure made up of regular hexagons, with interatomic distance 1.42 Å. Using Eq. (12) we have calculated the bond order (b.o.) for graphite. The calculation was performed on a PC using MAPLE V by Waterloo Maple Inc. and the result was b.o.$=0.5249$ (in units of β). The integrals of four variables in Eq. (15) were solved numerically using the function D01FCF of the Fortran library NAG MARK17 (a multidimensional adaptive deterministic quadrature over hyperrectangle).

Equations (1) and (2) would allow us to calculate the CC stretching interactions at any distance; but in fact there is a distance beyond which interactions become negligible. According to our calculations the interactions between CC bonds in graphite cease to be significant beyond the sixth nearest cell (we considered 10^{-3} mdyn/Å as the threshold). Furthermore, since we are integrating fast-oscillating functions, the precision of the result becomes very poor as the distance of interaction lengthens and the computation time needed to obtain meaningful results increases dramatically.

The force constants obtained have values that are compatible with the valence force fields that have already been calculated for other aromatic hydrocarbons: the value of the CC-stretching diagonal constants is 5.893 mdyn/Å. Furthermore the Kekulè rule[13] is satisfied on any path along the graphite bonds. In Fig. 3 we show the force constants on a *cis* path and on a *trans* path. The complete list of CC stretching valence force constants is reported in Table I.

B. Internal and symmetry coordinates treatment of graphite

Since the force field developed here is a valence force field, our treatment of normal modes of graphite is based on internal coordinates,[14,15] so that each mode is described by a linear combination of internal coordinates belonging to a specific symmetry species.[16] We have defined nine internal in-plane coordinates in the reference cell (see Fig. 2), thus obtaining $9N$ internal coordinates for the whole crystal (where N is the total number of cells in the lattice). On the other hand, the vibrational in-plane degrees of freedom of the lattice at each $\mathbf{k}\neq\mathbf{0}$ are only 4. This means that at $\mathbf{k}\neq\mathbf{0}$ the internal coordinates are not independent, but are linked by five relationships, called redundancies. Moreover, at Γ there are only two in-plane vibrational degrees of freedom so a total number of seven redundancies must be found.

In the graphite lattice there are three kinds of redundancies which arise, respectively, from the following three conditions: (i) During the vibration the sum of three valence angles with a common vertex must equal 2π. (ii) Each hexagonal ring must remain closed. (iii) The infinite crystal cannot increase further its dimensions.

Conditions (i) and (ii) yield five redundancy relations, each of which is a function of $\mathbf{k}$. Condition (iii) is always satisfied when $\mathbf{k}\neq\mathbf{0}$, so it must be explicitly set only at Γ (i.e., at $\mathbf{k}=\mathbf{0}$), thus giving the two additional conditions at point Γ. The seven redundancies of graphite, obtained with the method described in Ref. 17, are listed in Table II.

Having removed redundancies at the high symmetry points of the first Brillouin Zone (BZ) of graphite it becomes possible to obtain analytic expressions for nonredundant symmetry coordinates. At points Γ, K, and M the structure of the representation in the vibrational space is such that no more than one vibrational coordinate belongs to each species. This implies that after redundancies removal the symmetry coordinates obtained give directly the exact description of phonon eigenvectors in cell (0,0). In the following sections nonredundant symmetry coordinates for Γ, K, and M points are described.

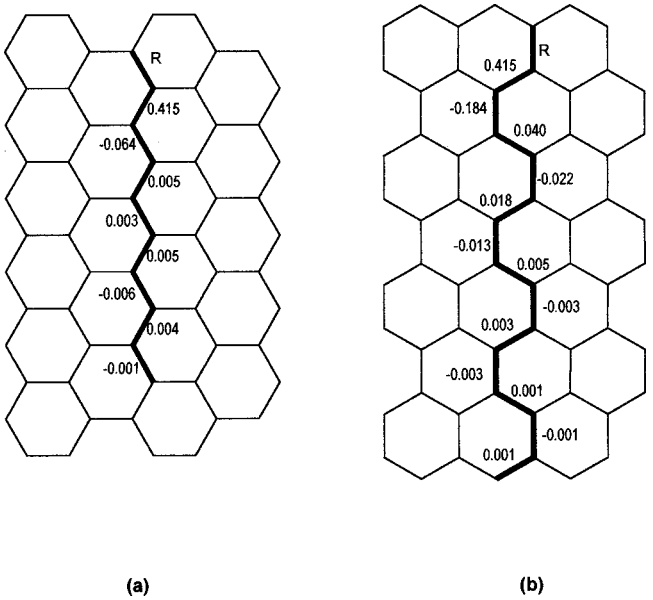

FIG. 3. Force constants of CC-stretching interaction between R and other CC bonds (a) on a *trans* path and (b) on a *cis* path.

TABLE I. List of the calculated force constants for graphite. Each row reports the interaction between CC bond number R_a of cell (0,0) and bond number R_b of cell (n_1,n_2).

R_a	R_b	n_1	n_2	Force const.	R_a	R_b	n_1	n_2	Force const.	R_a	R_b	n_1	n_2	Force const.	R_a	R_b	n_1	n_2	Force const.
1	1	−6	−3	−0.001	1	1	0	0	5.893	1	1	6	3	−0.001	2	2	−1	0	−0.064
1	1	−6	0	−0.001	1	1	0	1	−0.064	2	2	−9	6	−0.001	2	2	0	0	5.893
1	1	−6	3	−0.001	1	1	0	2	0.003	2	2	−6	6	−0.001	2	2	1	0	−0.064
1	1	−6	4	0.001	1	1	0	3	−0.006	2	2	−3	6	−0.001	2	2	2	0	0.003
1	1	−6	5	0.001	1	1	0	4	−0.001	2	2	−2	6	0.001	2	2	3	0	−0.006
1	1	−5	−2	−0.001	1	1	0	6	−0.001	2	2	−1	6	0.001	2	2	4	0	−0.001
1	1	−5	1	−0.002	1	1	1	−5	−0.002	2	2	−7	5	−0.001	2	2	6	0	−0.001
1	1	−5	3	0.001	1	1	1	−4	0.001	2	2	−4	5	−0.002	2	2	−4	−1	−0.002
1	1	−5	4	−0.001	1	1	1	−3	−0.002	2	2	−2	5	0.001	2	2	−3	−1	0.001
1	1	−5	5	0.001	1	1	1	−2	−0.22	2	2	−1	5	−0.001	2	2	−2	−1	−0.002
1	1	−5	6	0.001	1	1	1	−1	0.082	2	2	0	5	0.001	2	2	−1	−1	−0.022
1	1	−4	−4	−0.001	1	1	1	0	−0.064	2	2	1	5	0.001	2	2	0	−1	0.082
1	1	−4	−1	−0.002	1	1	1	1	−0.044	2	2	−8	4	−0.001	2	2	1	−1	−0.064
1	1	−4	0	−0.001	1	1	1	2	−0.005	2	2	−5	4	−0.002	2	2	2	−1	−0.044
1	1	−4	1	0.001	1	1	1	4	−0.002	2	2	−4	4	−0.001	2	2	3	−1	−0.005
1	1	−4	−2	−0.003	1	1	2	−4	−0.003	2	2	−3	4	0.001	2	2	5	−1	−0.002
1	1	−4	3	0.003	1	1	2	−3	0.006	2	2	−2	4	−0.003	2	2	−2	−2	−0.003
1	1	−4	4	0.002	1	1	2	−2	0.018	2	2	−1	4	0.003	2	2	−1	−2	0.006
1	1	−4	5	−0.001	1	1	2	−1	−0.022	2	2	0	4	0.002	2	2	0	−2	0.018
1	1	−4	6	0.001	1	1	2	0	0.003	2	2	1	4	−0.001	2	2	1	−2	−0.022
1	1	−3	−6	−0.001	1	1	2	1	−0.005	2	2	2	4	0.001	2	2	2	−2	0.003
1	1	−3	−3	−0.002	1	1	2	2	−0.007	2	2	−9	3	−0.001	2	2	3	−2	−0.005
1	1	−3	−2	−0.01	1	1	2	3	−0.001	2	2	−6	3	−0.002	2	2	4	−2	−0.007
1	1	−3	0	−0.006	1	1	2	5	−0.001	2	2	−5	3	−0.001	2	2	5	−2	−0.001
1	1	−3	1	−0.002	1	1	3	−6	−0.001	2	2	−3	3	−0.006	2	2	7	−2	−0.001
1	1	−3	2	0.006	1	1	3	−5	0.001	2	2	−2	3	−0.002	2	2	−3	−3	−0.001
1	1	−3	3	−0.002	1	1	3	−4	0.003	2	2	−1	3	0.006	2	2	−2	−3	0.001
1	1	−3	4	0.003	1	1	3	−3	−0.002	2	2	0	3	−0.002	2	2	−1	−3	0.003
1	1	−3	5	0.001	1	1	3	−2	0.006	2	2	1	3	0.003	2	2	0	−3	−0.002
1	1	−3	6	−0.001	1	1	3	−1	−0.002	2	2	2	3	0.001	2	2	1	−3	0.006
1	1	−2	−5	−0.001	1	1	3	0	−0.006	2	2	3	3	−0.001	2	2	2	−3	−0.002
1	1	−2	−3	−0.001	1	1	3	2	−0.001	2	2	−7	2	−0.001	2	2	3	−3	−0.006
1	1	−2	−2	−0.007	1	1	3	3	−0.002	2	2	−5	2	−0.001	2	2	5	−3	−0.001
1	1	−2	−1	−0.005	1	1	3	6	−0.001	2	2	−4	2	−0.007	2	2	6	−3	−0.002
1	1	−2	0	0.003	1	1	4	−6	0.001	2	2	−3	2	−0.005	2	2	9	−3	−0.001
1	1	−2	1	−0.022	1	1	4	−5	−0.001	2	2	−2	2	0.003	2	2	−2	−4	0.001
1	1	−2	2	0.018	1	1	4	−4	0.002	2	2	−1	2	−0.022	2	2	−1	−4	−0.001
1	1	−2	3	0.006	1	1	4	−3	0.003	2	2	0	2	0.018	2	2	0	−4	0.002
1	1	−2	4	−0.003	1	1	4	−2	−0.003	2	2	1	2	0.006	2	2	1	−4	0.003
1	1	−1	−4	−0.002	1	1	4	−1	0.001	2	2	2	2	−0.003	2	2	2	−4	−0.003
1	1	−1	−2	−0.005	1	1	4	0	−0.001	2	2	−5	1	−0.002	2	2	3	−4	0.001
1	1	−1	−1	−0.044	1	1	4	1	−0.002	2	2	−3	1	−0.005	2	2	4	−4	−0.001
1	1	−1	0	−0.064	1	1	4	4	−0.001	2	2	−2	1	−0.044	2	2	5	−4	−0.002
1	1	−1	1	0.082	1	1	5	−6	0.001	2	2	−1	1	−0.064	2	2	8	−4	−0.001
1	1	−1	2	−0.022	1	1	5	−5	0.001	2	2	0	1	0.082	2	2	−1	−5	0.001
1	1	−1	3	−0.002	1	1	5	−4	−0.001	2	2	1	1	−0.022	2	2	0	−5	0.001
1	1	−1	4	0.001	1	1	5	−3	0.001	2	2	2	1	−0.002	2	2	1	−5	−0.001
1	1	−1	5	−0.002	1	1	5	−1	−0.002	2	2	3	1	0.001	2	2	2	−5	0.001
1	1	0	−6	−0.001	1	1	5	2	−0.001	2	2	4	1	−0.002	2	2	4	−5	−0.002
1	1	0	−4	−0.001	1	1	6	−5	0.001	2	2	−6	0	−0.001	2	2	7	−5	−0.001
1	1	0	−3	−0.006	1	1	6	−4	0.001	2	2	−4	0	−0.001	2	2	1	−6	0.001
1	1	0	−2	0.003	1	1	6	−3	−0.001	2	2	−3	0	−0.006	2	2	2	−6	0.001
1	1	0	−1	−0.064	1	1	6	0	−0.001	2	2	−2	0	0.003	2	2	3	−6	−0.001

TABLE I. *(Continued).*

R_a	R_b	n_1	n_2	Force const.	R_a	R_b	n_1	n_2	Force const.	R_a	R_b	n_1	n_2	Force const.	R_a	R_b	n_1	n_2	Force const.
2	2	6	−6	−0.001	3	3	2	−2	0.003	3	3	3	3	−0.001	1	2	1	−2	−0.008
2	2	9	−6	−0.001	3	3	1	−1	−0.064	3	3	0	6	−0.001	1	2	1	−1	−0.184
3	3	3	−9	−0.001	3	3	0	0	5.893	3	3	−3	9	−0.001	1	2	1	0	0.415
3	3	0	−6	−0.001	3	3	−1	1	−0.064	1	2	−6	0	0.001	1	2	1	1	0.040
3	3	−3	−3	−0.001	3	3	−2	2	0.003	1	2	−6	2	0.001	1	2	1	2	−0.009
3	3	−4	−2	0.001	3	3	−3	3	−0.006	1	2	−6	3	0.001	1	2	1	4	0.001
3	3	−5	−1	0.001	3	3	−4	4	−0.001	1	2	−6	4	−0.001	1	2	1	5	−0.001
3	3	2	−7	−0.001	3	3	−6	6	−0.001	1	2	−5	−2	0.001	1	2	2	−6	−0.001
3	3	−1	−4	−0.002	3	3	5	−4	−0.002	1	2	−5	0	0.001	1	2	2	−4	−0.001
3	3	−3	−2	0.001	3	3	4	−3	0.001	1	2	−5	1	0.001	1	2	2	−3	−0.013
3	3	−4	−1	−0.001	3	3	3	−2	−0.002	1	2	−5	3	0.001	1	2	2	−2	−0.008
3	3	−5	0	0.001	3	3	2	−1	−0.022	1	2	−5	5	−0.001	1	2	2	−1	0.040
3	3	−6	1	0.001	3	3	1	0	0.082	1	2	−4	−2	0.001	1	2	2	0	0.005
3	3	4	−8	−0.001	3	3	0	1	−0.064	1	2	−4	−1	0.001	1	2	2	1	0.018
3	3	1	−5	−0.002	3	3	−1	2	−0.044	1	2	−4	1	0.002	1	2	2	2	0.005
3	3	0	−4	−0.001	3	3	−2	3	−0.005	1	2	−4	2	0.003	1	2	2	3	−0.002
3	3	−1	−3	0.001	3	3	−4	5	−0.002	1	2	−4	3	−0.002	1	2	3	−5	−0.003
3	3	−2	−2	−0.003	3	3	4	−2	−0.003	1	2	−4	4	0.001	1	2	3	−4	−0.001
3	3	−3	−1	0.003	3	3	3	−1	0.006	1	2	−4	6	−0.001	1	2	3	−3	0.002
3	3	−4	0	0.002	3	3	2	0	0.018	1	2	−3	−3	0.001	1	2	3	−2	−0.009
3	3	−5	1	−0.001	3	3	1	1	−0.022	1	2	−3	−1	0.002	1	2	3	−1	0.018
3	3	−6	2	0.001	3	3	0	2	0.003	1	2	−3	0	0.004	1	2	3	0	0.005
3	3	6	−9	−0.001	3	3	−1	3	−0.005	1	2	−3	2	0.005	1	2	3	2	0.003
3	3	3	−6	−0.002	3	3	−2	4	−0.007	1	2	−3	4	−0.003	1	2	3	3	0.001
3	3	2	−5	−0.001	3	3	−3	5	−0.001	1	2	−2	−4	−0.001	1	2	3	4	−0.001
3	3	0	−3	−0.006	3	3	−5	7	−0.001	1	2	−2	−3	0.001	1	2	4	−4	−0.003
3	3	−1	−2	−0.002	3	3	6	−3	−0.001	1	2	−2	−2	0.003	1	2	4	−2	0.005
3	3	−2	−1	0.006	3	3	5	−2	0.001	1	2	−2	0.	0.005	1	2	4	0	0.004
3	3	−3	0.	−0.002	3	3	4	−1	0.003	1	2	−2	1	0.018	1	2	4	1	0.002
3	3	−4	1	0.003	3	3	3	0	−0.002	1	2	−2	2	−0.009	1	2	4	3	0.001
3	3	−5	2	0.001	3	3	2	1	0.006	1	2	−2	3	0.002	1	2	5	−6	−0.001
3	3	−6	3	−0.001	3	3	1	2	−0.002	1	2	−2	4	−0.001	1	2	5	−4	0.001
3	3	5	−7	−0.001	3	3	0	3	−0.006	1	2	−2	5	−0.003	1	2	5	−3	−0.002
3	3	3	−5	−0.001	3	3	−2	5	−0.001	1	2	−1	−3	−0.002	1	2	5	−2	0.003
3	3	2	−4	−0.007	3	3	−3	6	−0.002	1	2	−1	−2	0.005	1	2	5	−1	0.002
3	3	1	−3	−0.005	3	3	−6	9	−0.001	1	2	−1	−1	0.018	1	2	5	1	0.001
3	3	0	−2	0.003	3	3	6	−2	0.001	1	2	−1	0	0.005	1	2	5	2	0.001
3	3	−1	−1	−0.022	3	3	5	−1	−0.001	1	2	−1	1	0.040	1	2	6	−5	−0.001
3	3	−2	0	0.018	3	3	4	0	0.002	1	2	−	2	−0.008	1	2	6	−3	0.001
3	3	−3	1	0.006	3	3	3	1	0.003	1	2	−1	3	−0.013	1	2	6	−1	0.001
3	3	−4	2	−0.003	3	3	2	2	−0.003	1	2	−1	4	−0.001	1	2	6	0	0.001
3	3	4	−5	−0.002	3	3	1	3	0.001	1	2	−1	6	−0.001	1	2	6	2	0.001
3	3	2	−3	−0.005	3	3	0	4	−0.001	1	2	0	−5	−0.001	1	2	7	−4	−0.001
3	3	1	−2	−0.044	3	3	−1	5	−0.002	1	2	0	−4	0.001	1	2	7	−3	0.001
3	3	0	−1	−0.064	3	3	−4	8	−0.001	1	2	0	−2	−0.009	1	2	7	−2	0.001
3	3	−1	0	0.082	3	3	6	−1	0.001	1	2	0	−1	0.040	1	2	7	0	0.001
3	3	−2	1	−0.022	3	3	5	0	0.001	1	2	0	0	0.415	1	3	0	−6	0.001
3	3	−3	2	−0.002	3	3	4	1	−0.001	1	2	0	1	−0.184	1	3	2	−6	0.001
3	3	−4	3	0.001	3	3	3	2	0.001	1	2	0	2	−0.008	1	3	3	−6	0.001
3	3	−5	4	−0.002	3	3	1	4	−0.002	1	2	0	3	0.002	1	3	4	−6	−0.001
3	3	6	−6	−0.001	3	3	−2	7	−0.001	1	2	0	4	−0.003	1	3	−2	−5	0.001
3	3	4	−4	−0.001	3	3	5	1	0.001	1	2	1	−4	−0.003	1	3	0	−5	0.001
3	3	3	−3	−0.006	3	3	4	2	0.001	1	2	1	−3	0.002	1	3	1	−5	0.001
1	3	3	−5	0.001	1	3	2	1	−0.009	2	3	5	−5	0.001	2	3	−1	1	0.415

TABLE I. *(Continued).*

R_a	R_b	n_1	n_2	Force const.	R_a	R_b	n_1	n_2	Force const.	R_a	R_b	n_1	n_2	Force const.	R_a	R_b	n_1	n_2	Force const.
1	3	5	−5	−0.001	1	3	4	1	0.001	2	3	4	−5	0.001	2	3	−2	1	0.040
1	3	−2	−4	0.001	1	3	5	1	−0.001	2	3	2	−5	0.001	2	3	−3	1	−0.009
1	3	−1	−4	0.001	1	3	−6	2	−0.001	2	3	0	−5	−0.001	2	3	−5	1	0.001
1	3	1	−4	0.002	1	3	−4	2	−0.001	2	3	6	−4	0.001	2	3	−6	1	−0.001
1	3	2	−4	0.003	1	3	−3	2	−0.013	2	3	5	−4	0.001	2	3	4	2	−0.001
1	3	3	−4	−0.002	1	3	−2	2	−0.008	2	3	3	−4	0.002	2	3	2	2	−0.001
1	3	4	−4	0.001	1	3	−1	2	0.040	2	3	2	−4	0.003	2	3	1	2	−0.013
1	3	6	−4	−0.001	1	3	0	2	0.005	2	3	1	−4	−0.002	2	3	0	2	−0.008
1	3	−3	−3	0.001	1	3	1	2	0.018	2	3	0	−4	0.001	2	3	−1	2	0.040
1	3	−1	−3	0.002	1	3	2	2	0.005	2	3	−2	−4	−0.001	2	3	−2	2	0.005
1	3	0	−3	0.004	1	3	3	2	−0.002	2	3	6	−3	0.001	2	3	−3	2	0.018
1	3	2	−3	0.005	1	3	−5	3	−0.003	2	3	4	−3	0.002	2	3	−4	2	0.005
1	3	4	−3	−0.003	1	3	−4	3	−0.001	2	3	3	−3	0.004	2	3	−5	2	−0.002
1	3	−4	−2	−0.001	1	3	−3	3	0.002	2	3	1	−3	0.005	2	3	2	3	−0.003
1	3	−3	−2	0.001	1	3	−2	3	−0.009	2	3	−1	−3	−0.003	2	3	1	3	−0.001
1	3	−2	−2	0.003	1	3	−1	3	0.018	2	3	6	−2	−0.001	2	3	0	3	0.002
1	3	0	−2	0.005	1	3	0	3	0.005	2	3	5	−2	0.001	2	3	−1	3	−0.009
1	3	1	−2	0.018	1	3	2	3	0.003	2	3	4	−2	0.003	2	3	−2	3	0.018
1	3	2	−2	−0.009	1	3	3	3	0.001	2	3	2	−2	0.005	2	3	−3	3	0.005
1	3	3	−2	0.002	1	3	4	3	−0.001	2	3	1	−2	0.018	2	3	−5	3	0.003
1	3	4	−2	−0.001	1	3	−4	4	−0.003	2	3	0	−2	−0.009	2	3	−6	3	0.001
1	3	5	−2	−0.003	1	3	−2	4	0.005	2	3	−1	−2	0.002	2	3	−7	3	−0.001
1	3	−3	−1	−0.002	1	3	0	4	0.004	2	3	−2	−2	−0.001	2	3	0	4	−0.003
1	3	−2	−1	0.005	1	3	1	4	0.002	2	3	−3	−2	−0.003	2	3	−2	4	0.005
1	3	−1	−1	0.018	1	3	3	4	0.001	2	3	4	−1	−0.002	2	3	−4	4	0.004
1	3	0	−1	0.005	1	3	−6	5	−0.001	2	3	3	−1	0.005	2	3	−5	4	0.002
1	3	1	−1	0.040	1	3	−4	5	0.001	2	3	2	−1	0.018	2	3	−7	4	0.001
1	3	2	−1	−0.008	1	3	−3	5	−0.002	2	3	1	−1	0.005	2	3	1	5	−0.001
1	3	3	−1	−0.013	1	3	−2	5	0.003	2	3	0	−1	0.040	2	3	−1	5	0.001
1	3	4	−1	−0.001	1	3	−1	5	0.002	2	3	−1	−1	−0.008	2	3	−2	5	−0.002
1	3	6	−1	−0.001	1	3	1	5	0.001	2	3	−2	−1	−0.013	2	3	−3	5	0.003
1	3	−5	0	−0.001	1	3	2	5	0.001	2	3	−3	−1	−0.001	2	3	−4	5	0.002
1	3	−4	0	0.001	1	3	−5	6	−0.001	2	3	−5	−1	−0.001	2	3	−6	5	0.001
1	3	−2	0	−0.009	1	3	−3	6	0.001	2	3	5	0	−0.001	2	3	−7	5	0.001
1	3	−1	0	0.0040	1	3	−1	6	0.001	2	3	4	0	0.001	2	3	−1	6	−0.001
1	3	0	0	0.415	1	3	0	6	0.001	2	3	2	0	−0.009	2	3	−3	6	0.001
1	3	1	0	−0.184	1	3	2	6	0.001	2	3	1	0	0.040	2	3	−5	6	0.001
1	3	2	0	−0.008	1	3	−4	7	−0.001	2	3	0	0	0.415	2	3	−6	6	0.001
1	3	3	0	0.002	1	3	−3	7	0.001	2	3	−1	0	−0.184	2	3	−8	6	0.001
1	3	4	0	−0.003	1	3	−2	7	0.001	2	3	−2	0	−0.008	2	3	−3	7	−0.001
1	3	−4	1	−0.003	1	3	0	7	0.001	2	3	−3	0	0.002	2	3	−4	7	0.001
1	3	−3	1	0.002	2	3	6	−6	0.001	2	3	−4	0	−0.003	2	3	−5	7	0.001
1	3	−2	1	−0.008	2	3	4	−6	0.001	2	3	3	1	−0.003	2	3	−7	7	0.001
1	3	−1	1	−0.184	2	3	3	−6	0.001	2	3	2	1	0.002					
1	3	0	1	0.415	2	3	2	−6	−0.001	2	3	1	1	−0.008					
1	3	1	1	0.040	2	3	7	−5	0.001	2	3	0	1	−0.184					

1. **Γ** *point*

In-plane structure of the representation:

$$\Gamma_{\text{tot,in-plane}} = E_{1u} + E_{2g}.$$

Translations along x and y belong to E_{1u}, thus leaving only a twofold degenerate E_{2g} vibrational mode.

Redundancies:

(a) Local redundancies Π_1, Π_2 as in Table II.

(b) Ring redundancies

$$\Pi_3 = \Sigma_i \omega_i + \Sigma_i \omega_i' = 0,$$

$$\Pi_4 = \omega_1 + 2\omega_3 + \omega_1' + 2\omega_2' = 0,$$

$$\Pi_5 = 3\omega_1 - \omega_1' + 2\omega_2' + 2\omega_3' = 0.$$

(c) Crystal redundancies Π_6, Π_7 as in Table II.

TABLE II. General expression of the vibrational redundancies of a single planar sheet of graphite. R_{CC} is the CC bond length at equilibrium in Å.

(a) Local redundancies:	$\Pi_1=\Sigma_i\omega_i=0$
	$\Pi_2=\Sigma_i\omega_i'=0$
(b) Ring redundancies:	$\Pi_3=\omega_1+\omega_2e^{i\theta_1}+\omega_3e^{i\theta_2}+\omega_1'e^{i(\theta_1+\theta_2)}+\omega_2'e^{i\theta_2}+\omega_3'e^{i\theta_1}=0$
	$\Pi_4=2R_1(e^{i\theta_1}-e^{i\theta_2})+R_2(1-e^{i\theta_2})-R_3(1-e^{i\theta_1})-\sqrt{3}R_{CC}(\omega_1+2\omega_3e^{i\theta_2}+\omega_1'e^{i(\theta_1+\theta_2)}+2\omega_2'e^{i\theta_2})=0$
	$\Pi_5=\sqrt{3}[R_2(1-e^{i\theta_2})+R_3(1-e^{i\theta_1})]+R_{CC}(3\omega_1-\omega_1'e^{i(\theta_1+\theta_2)}+2\omega_2'e^{i\theta_2}+2\omega_3'e^{i\theta_1})=0$
(c) Crystal redundancies: (only at Γ)	$\Pi_6=\Sigma_iR_i=0$
	$\Pi_7=\sqrt{3}(R_2+R_3)-R_{CC}(\omega_2+\omega_3)=0$

Removing redundancies[15] yields the following symmetry coordinates:

$$E_{2g}:\quad \mathcal{R}_x=R_{CC}(2R_1-R_2-R_3)+\frac{\sqrt{3}}{2}(2\omega_1-\omega_2-\omega_3+2\omega_1'-\omega_2'-\omega_3'),$$

$$\mathcal{R}_y=R_{CC}(R_2-R_3)+\frac{\sqrt{3}}{2}(\omega_2-\omega_3+\omega_2'-\omega_3'),$$

where R_{CC} denotes the CC bond length.

Notice that the crystal redundancies (Π_6 and Π_7) belong to E_{2g} species; combining them one can obtain the redundancies iso-oriented with the E_{2g} $\mathcal{R}$ coordinates.

$$\Pi_x=\sqrt{3}(2R_1-R_2-R_3)-R_{CC}(2\omega_1-\omega_2-\omega_3),$$

$$\Pi_y=\sqrt{3}(R_2-R_3)-R_{CC}(\omega_2-\omega_3).$$

2. K point (D_{3h} point symmetry)

In-plane structure of the representation:

$$\Gamma_{\text{tot,in-plane}}=A_1'+A_2'+E.$$

Redundancies:
(a) Local redundancies Π_1,Π_2 as in Table II.
(b) Ring redundancies

$$\Pi_3=\omega_1+\omega_2e^{i(4/3)\pi}+\omega_3e^{i(2/3)\pi}+\omega_1'+\omega_2'e^{i(2/3)\pi}+\omega_3'e^{i(4/3)\pi}=0,$$

$$\Pi_4=2R_1-R_2e^{i(4/3)\pi}-R_3e^{i(2/3)\pi}-\frac{R_{CC}}{\sqrt{3}}(2\omega_1-\omega_2e^{i(4/3)\pi}-\omega_3e^{i(2/3)\pi}+2\omega_1'-\omega_2'e^{i(2/3)\pi}-\omega_3'e^{i(4/3)\pi})=0,$$

$$\Pi_5=\sqrt{3}[R_2(1-e^{i(2/3)\pi})+R_3(1-e^{i(4/3)\pi})]+R_{CC}(3\omega_1-\omega_1'+2\omega_2'e^{i(2/3)\pi}+2\omega_3'e^{i(4/3)\pi})=0.$$

Combining the nine internal coordinates according to the character table of D_{3h} point group one obtains nine symmetry coordinates. These coordinates are not linearly independent because they are linked by the five redundancies.

We list the symmetry coordinates after removal of the redundancies:

Species	Coordinate
A_1'	$S_1=R_1+R_2e^{i(4/3)\pi}+R_3e^{i(2/3)\pi}$
A_2'	$S_2=\omega_1+\omega_2e^{i(4/3)\pi}+\omega_3e^{i(2/3)\pi}-\omega_1'-\omega_2'e^{i(2/3)\pi}-\omega_3'e^{i(4/3)\pi}$
E'	$S_{3x}=(2R_1-R_2e^{i(4/3)\pi}-R_3e^{i(2/3)\pi})+\sqrt{3}/R_{CC}[(2\omega_1-\omega_2e^{i(4/3)\pi}-\omega_3e^{i(2/3)\pi})+(2\omega_1'-\omega_2'e^{i(2/3)\pi}-\omega_3'e^{i(4/3)\pi})]$.

3. M point (D_{2h} point symmetry)

In-plane structure of the representation:

$$\Gamma_{\text{tot,in-plane}}=A_g+B_{1g}+B_{2u}+B_{3u}.$$

Redundancies:
(a) Local redundancies Π_1, Π_2 as in Table II.
(b) Ring redundancies

$$\Pi_3=\omega_1-\omega_2-\omega_3+\omega_1'-\omega_2'-\omega_3'=0,$$

$$\Pi_4=2(R_2-R_3)-\sqrt{3}R_{CC}(\omega_1+2\omega_3+\omega_1'-2\omega_2')=0,$$

$$\Pi_5=2\sqrt{3}(R_2+R_3)+R_{CC}(3\omega_1-\omega_1'-2\omega_2'-2\omega_3')=0.$$

Symmetry coordinates (after removal of the redundancies):

Species	Coordinate
A_g	$S_1 = R_1$
B_{1g}	$S_2 = (\omega_2 + \omega_2') - (\omega_3 + \omega_3')$
B_{2u}	$S_3 = \sqrt{3} R_{CC}(R_2 - R_3) + 2[(\omega_2 - \omega_3) - (\omega_2' - \omega_3')]$
B_{3u}	$S_4 = R_{CC}(R_2 + R_3) - 2\sqrt{3}[(\omega_2 + \omega_3) - (\omega_2' + \omega_3')]$

C. Phonons of graphite

Using our force field we have calculated numerically both the phonon dispersion curves in the three symmetry directions of the reciprocal lattice of graphite (Γ-*K*, *K*-*M*, and *M*-Γ) and the corresponding one-phonon density of states (DOS). We have also plotted the shape of the normal modes at Γ, *M*, and *K* points. These results are shown in Figs. 4–6.

Notice that, according to the discussion in the previous sections, the nuclear displacements during normal modes at high-symmetry **k** values can be directly derived on the basis of the symmetry analysis, since only one normal mode per species is expected for Γ, *M*, and *K* points. As a consequence, the shape of the normal modes in Fig. 6 is independent of the force field. Conversely, the calculated frequency of the mode depends on the force field.

The agreement between our results and the experimental data is very satisfactory. In Fig. 4 the theoretical phonon dispersion curves are compared with experimental points obtained by electron-energy-loss spectroscopy[18] (EELS) and neutron scattering.[19] The agreement is excellent, especially at low frequencies. At high frequencies, in particular towards the center of the Brillouin zone, our force field gives frequencies that are lower with respect to the experimental data. The calculated frequency of the E_{2g} mode at Γ is 1541 cm^{-1}, while the experimental Raman value[20] is 1581 cm^{-1}. Nevertheless, the virtue of our field is the fact of being an extension of the MO/8 field also used for finite molecules without any variation of its parameters. Our aim was in fact to obtain, without any fitting procedure, a force field that could predict experimental data reasonably well and that would allow us to treat on common grounds graphite and molecular models. This will permit us to establish a correlation between the spectra of graphite and of PAH's of any size, as will be discussed in Sec. IV.

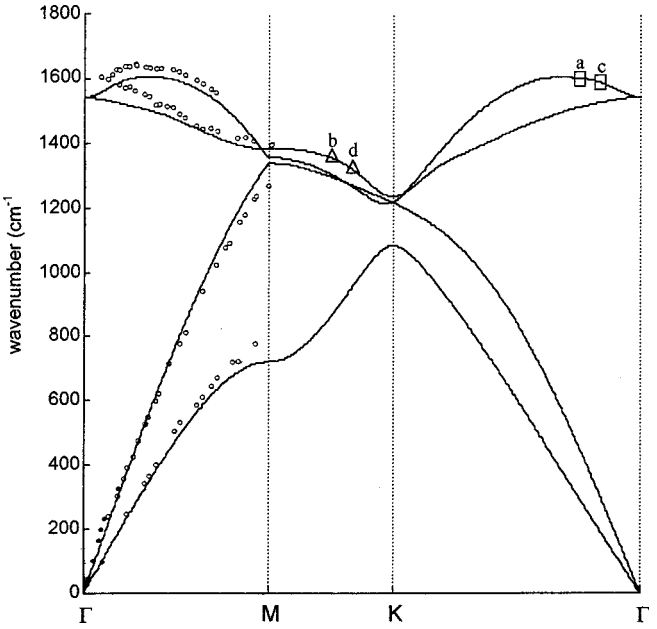

FIG. 4. Calculated phonon dispersion curves along three high-symmetry directions in the reciprocal lattice of graphite. Circles represent experimental data from EELS (empty circles) and neutron scattering (filled circles). Squares and triangles identify phonons that reproduce, respectively, Я and ♂ motions of coronene and HBC.

Several dispersion curves for graphite have been obtained in the literature. Some of them have been published by Dresselhaus and co-workers. Those presented in Ref. 21 show remarkable differences from those here reported: in particular the overall shape of the higher optical branches is very different in the Γ-*M* direction and these branches are much more apart. These curves have been modified in a following paper[22] to fit neutron-scattering data, thus obtaining a behavior more similar to that of our branches. Major differences can still be noticed along the *M*-*K* direction but unfortunately no direct experimental evidence can definitely choose the better behavior. A better resemblance can be found with curves by Kresse, Furthmüller, and Hafner,[23] which are based on an *ab initio* calculation of graphite electronic structure. This can be ascribed to the close analogy between their approach and ours. Notice that neither Kresse, Furthmüller, and Hafner nor we have performed any fitting on experimental data of graphite.

IV. COMPARISON WITH PAH's

Using Ohno's force field we carried out normal modes calculations on the molecules of coronene and hexabenzocoronene (Fig. 7) on the basis of the symmetry coordinates suitably constructed. Figure 8 shows the Raman spectra of solid samples of coronene and hexabenzocoronene (HBC) together with the plots of the motions which are assigned to the most relevant Raman lines. It becomes apparent that the strong lines in the Raman spectrum originate from two kinds of motion: one will be called Я and the other, which is a total symmetric breathing mode, will be called ♂. The label Я is the same one that was previously used for a normal mode, calculated and observed, of polyacetylene and poly-

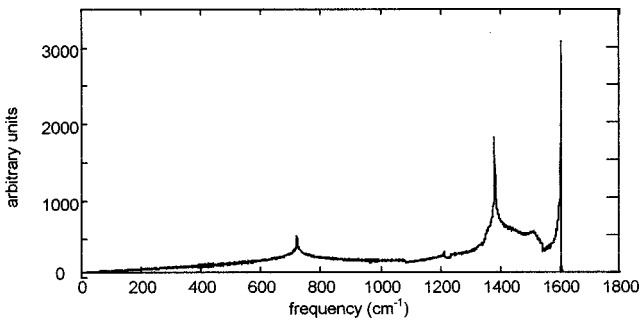

FIG. 5. One phonon density of vibrational states for a two-dimensional graphene sheet.

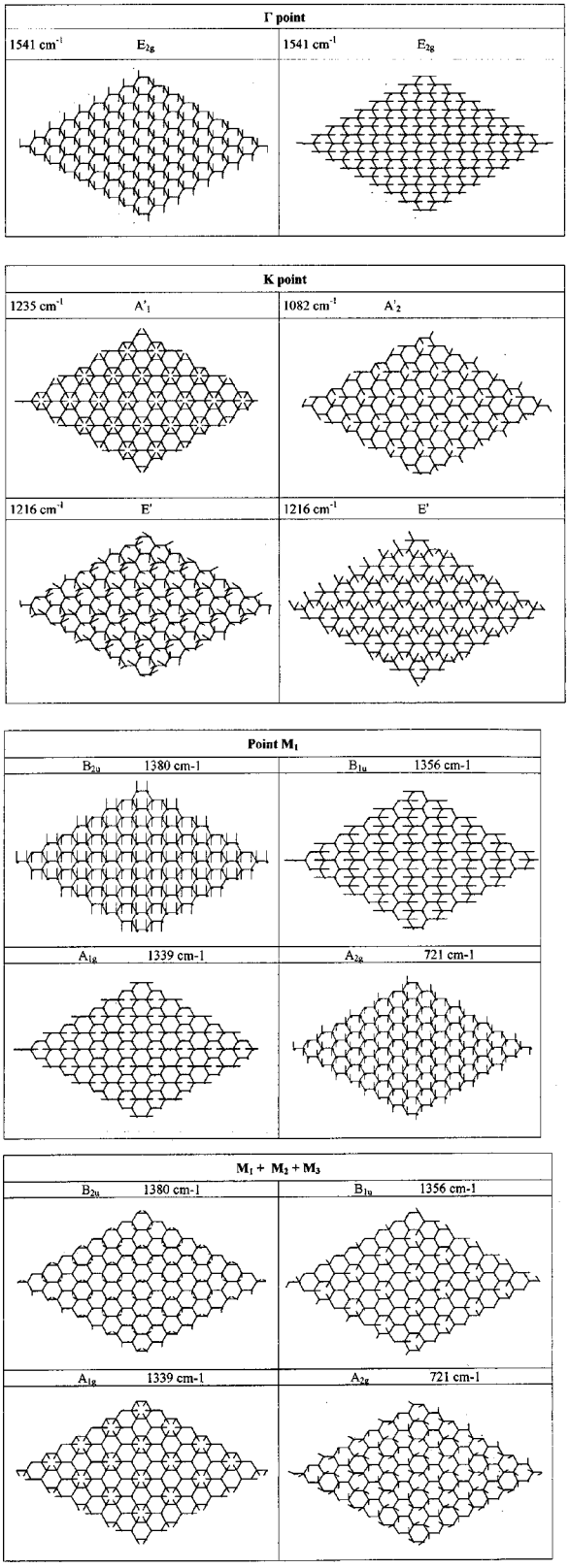

FIG. 6. Eigenvectors of graphite at points Γ, *K*, and *M* of the first BZ.

aromatic polymers. This motion, which has strong analogies with the E_{2g} mode of graphite, gives rise to an extremely strong line in the Raman spectrum of polyconjugated polymers.[24]

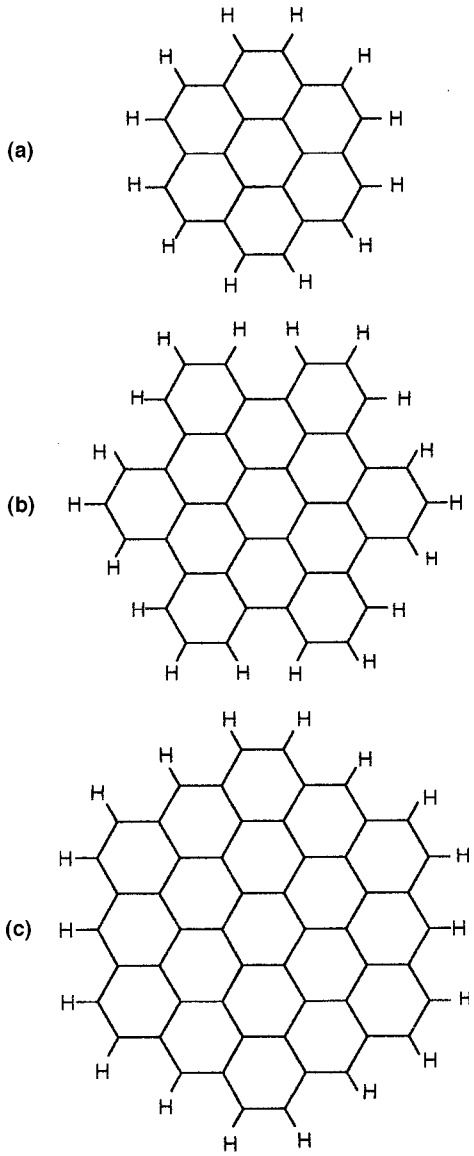

FIG. 7. The molecular structure of (a) coronene, (b) hexabenzocoronene (HBC), and (c) circumcoronene.

A comparison of Figs. 6 and 8 shows that the Я mode is obviously analogous to the only Raman active mode of graphite (the E_{2g} mode at Γ), which will thus be labeled as ''the Я mode'' of graphite. The ɑ motion of coronene and HBC is a totally symmetric mode and may thus be compared to the totally symmetric phonons of graphite at symmetry points *M* or *K* of the first BZ.

The analogy between the two Я modes (of graphite and of finite molecules) is not only intuitive but it has also been proved by a calculation, as shown below. We have used the same procedure in order to establish the degree of resemblance of the totally symmetric modes of graphite and of the ɑ mode of the oligomers. This procedure is described in detail in what follows.

A phonon is a traveling wave, while the normal mode of a finite domain can be approximately described[25] as a stationary wave. A stationary wave can be obtained from a phonon having wave vector **k** by summation with a phonon having wave vector $-\mathbf{k}$ and same frequency. In the case

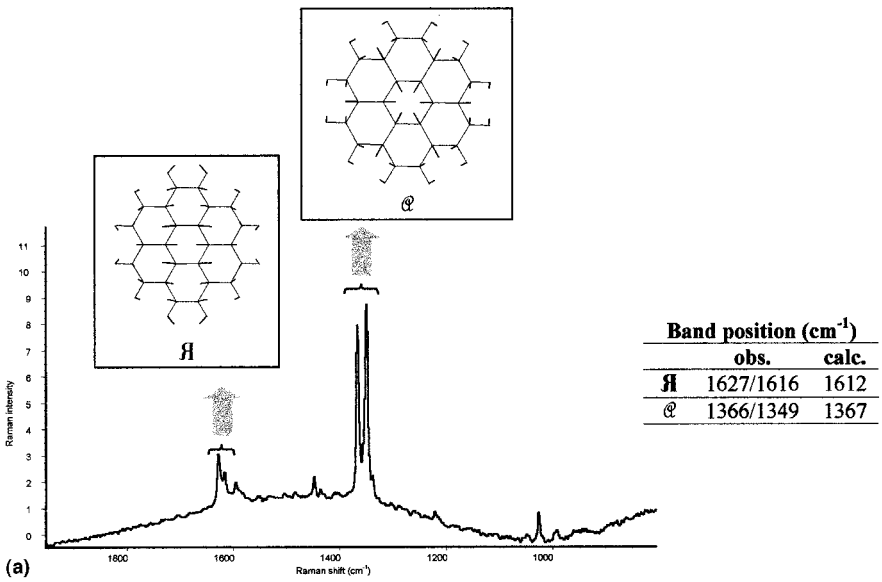

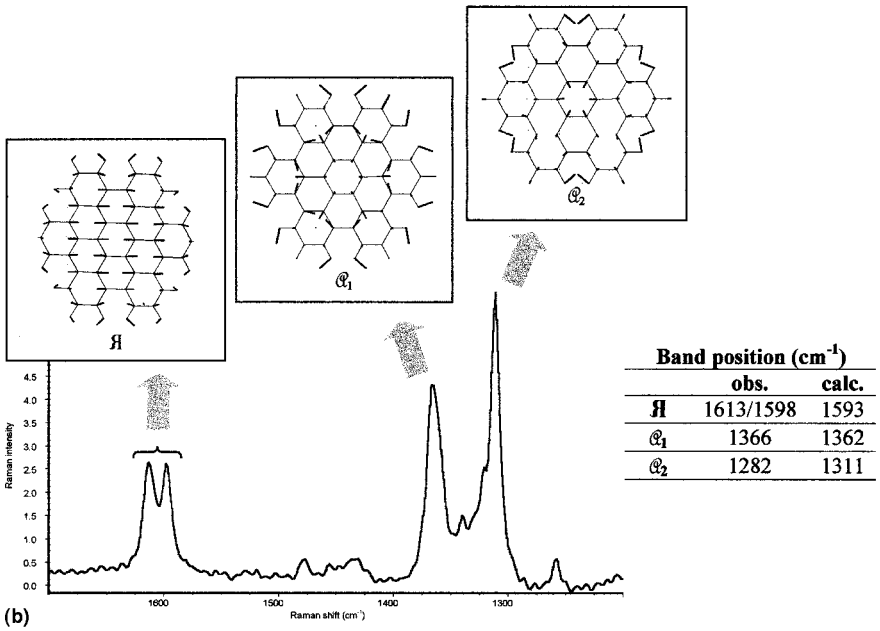

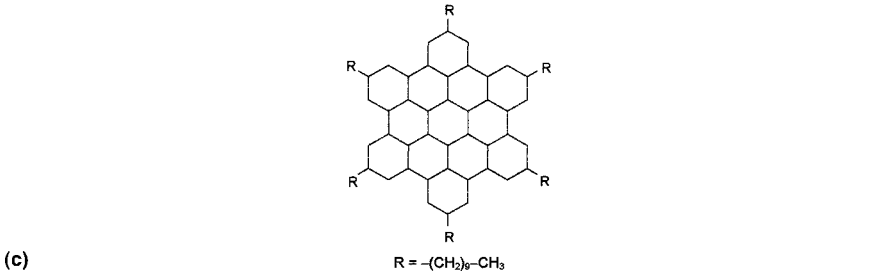

FIG. 8. Raman spectra of (a) coronene and (b) hexa-*peri*-hexabenzocoronene [substituent *R* groups as in figure (c)]. For the sake of simplicity we report the eigenvectors of the parent molecule without alkyl substituents. Spectrum (a) was obtained using $\lambda_{exc}=1064$ nm and spectrum (b) was obtained with $\lambda_{exc}=514.5$ nm.

under study we are dealing with phonons at points Γ, *K*, and *M* of the first BZ of graphite.

Phonons at Γ ($\mathbf{k}=\mathbf{0}$) are stationary waves and can be classified according to the D_{6h} point symmetry, therefore they can be directly compared with the $\mathit{Я}$ modes of finite molecules (we are considering coronene and HBC, with D_{6h} symmetry).

For any oligomer the ideal $\mathit{Я}$ motion is given by a collective coordinate $\mathit{Я}=\tilde{\mathbf{U}}_{\mathit{Я}}\mathbf{R}$ where $\mathbf{R}$ is a column vector which contains all the internal coordinates of the molecule considered and $\mathbf{U}_{\mathit{Я}}$ is the vector of the coefficients of the combination. In order to build $\mathbf{U}_{\mathit{Я}}$, a piece of graphite is considered which has the same shape as the molecules under investigation. Then the coefficient of the combination for

TABLE III. Raman spectrum of coronene: vibrational assignments and calculated ideal motions contents for coronene E_{2g} modes.

Sym. spec.	Calc. freq. (cm^{-1})	Obs. freq. (cm^{-1})	% of Я vibration	Weighted content of Я vibration
E_{2g}	3057		15	0.7701
	3056		19	0.6593
	1612	1627/1616 s	83	5.0454
	1439	1448 vw	35	1.6711
	1438		41	2.6904
	1396		0	0.0127
	1216	1223 vw	38	1.5189
	1149		24	1.7191
	997	994 vw	12	0.5067
	673		29	0.9573
	534		17	0.5309
	354	369 m	58	0.9816

each stretching or bending coordinate of the oligomer is taken equal to the coefficient of the Я symmetry coordinate of graphite crystal for the corresponding stretching or bending. We recall that the Я coordinate of graphite is the E_{2g} symmetry coordinate at point Γ, which is obtained summing on all the cells the symmetry coordinate of cell (0,0) times the corresponding phase factor (see note 16).

The scalar product between $\mathbf{U}_{Я}$ and each of the eigenvectors $\mathbf{L}_i$ (normalized to unity) of the oligomer equals 1 if the two vectors are equal and 0 if the two vectors are orthogonal. Therefore the meaning of such product is that of the ''content'' of Я motion in the ith eigenvector of the oligomer.

$$Я_{\%\text{content},i} = 100(\tilde{\mathbf{U}}_{Я} \cdot \mathbf{L}_i),$$

where $\mathbf{L}_i$ is the ith column of the eigenvectors matrix, $\mathbf{L}$. The molecular eigenvectors that we use in this product are normalized to unity, i.e., $\tilde{\mathbf{L}}_i \mathbf{L}_i = 1$.

On the other hand, Raman intensities are determined by

$$\frac{\partial \underline{\underline{\alpha}}}{\partial Q_i} = \sum_t \frac{\partial \underline{\underline{\alpha}}}{\partial R_t} L_{ti},$$

where L_{ti} is the tth element of $\boldsymbol{L}_i$, the eigenvector obtained by normalizing the eigenvectors matrix according to Wilson's procedure (i.e., $\boldsymbol{L}\tilde{\boldsymbol{L}} = \mathbf{G}$).

If we want to analyze Raman intensities in terms of the Я content, we have to use eigenvectors normalized with Wilson's method. The scalar product $\tilde{\mathbf{U}}_{Я} \cdot \boldsymbol{L}_i$ is a number that represents an amount of motion that is weighted by the effective mass of the ith oscillator; therefore this product allows for (i) the geometrical similarity between the ideal motion and the real eigenvector and (ii) the contribution of the eigenvector to Raman intensity. The calculated contents for coronene and HBC are listed in Tables III and IV. There is an immediate correlation between strong lines in the spectrum and modes with high Я content.

TABLE IV. Raman spectrum of HBC: vibrational assignments and calculated ideal motions contents for E_{2g} modes.

Sym. spec.	Calc. freq. (cm^{-1})	Obs. freq. (cm^{-1})	% of Я vibration	Weighted content of Я vibration
E_{2g}	3058		2	0.0225
	3057		6	0.0639
	3055		7	0.0716
	1607		2	0.0201
	1593	1605	87	0.8834
	1526		2	0.0224
	1475		9	0.0869
	1449		8	0.0903
	1335		12	0.1156
	1281		0	0.0021
	1249		6	0.0476
	1183		5	0.0502
	1100		5	0.0367
	1076		1	0.0053
	897		13	0.0854
	846		19	0.0858
	655		11	0.0597
	527		7	0.0249
	283		30	0.0543
	270		60	0.1062

Phonons at K are traveling waves that can be classified according to D_{3h} symmetry. In order to obtain stationary waves, we sum $\mathbf{k}$ and $-\mathbf{k}$ phonons. It can be shown that the stationary waves so obtained obey D_{6h} symmetry, so they are consistent with the normal modes of the finite domains. The eigenvector of the stationary wave so obtained has been used, by means of the same procedure described above for the Я motion, to build the ideal coordinate of totally symmetric K motion for each domain. We have then defined the vector $\mathbf{U}_K$ and computed the % motion content and the weighted motion content of the totally symmetric mode at point K in the A_{1g} normal modes of coronene and HBC. The results are shown in Tables V and VI.

Phonons at M are traveling waves with D_{2h} symmetry. It can be shown that[26(a)] a stationary wave that can be classified according to the D_{6h} point group may be obtained by summing the six degenerate phonons at points M_1, M_2, M_3 and $-M_1, -M_2, -M_3$. We have then built the $\mathbf{U}_M$ vector for coronene and for HBC and we have computed the contents of totally symmetric motion at M in the A_{1g} normal modes of coronene and HBC. The results are listed in Tables V and VI.

Figure 9 clearly shows that a large content of M motion does not produce strong lines in the Raman spectrum; on the contrary a large content of K motion is associated with strong lines in the Raman spectrum.

We have thus shown that the few strong Raman lines of the oligomers are due to motions which are related to the E_{2g} mode at Γ and to the A_1' phonon at K of graphite. These conclusions are in good agreement with the work of Yoshizawa *et al.*[27] based on semiempirical molecular orbital (MO) calculations on a few PAH molecules.

TABLE V. Raman spectrum of coronene: vibrational assignments and calculated ideal motions contents for coronene A_{1g} modes.

Sym. spec.	Calc. freq. (cm^{-1})	Obs. freq. (cm^{-1})	% of K vibration	Weighted content of K vibration	% of M vibration	Weighted content of M vibration
A_{1g}	3058	3042	1	0.0386	0	0.0052
	1599	1595 vw	8	0.4087	17	0.8663
	1367	1366/1349 vs	56	1.2514	5	0.1064
	1198		0	0.0153	10	0.5262
	1047	1025	2	0.0695	13	0.5009
	477	485 m	3	0.0207	13	0.0956

In this paper we analyze only coronene and HBC. We have also recorded the Raman spectra of many other PAH's, which have different size and well-defined shape,[28] and we have observed that the features of the spectra are the same for any PAH.[26] The strongest Raman lines are the $\mathcal{H}$ line around 1600 cm^{-1} and one or more strong lines near 1350 cm^{-1} are also observed. These latter lines are due to $\mathfrak{a}$ motion of the bulk, differently coupled with the end groups.

The frequencies of $\mathcal{H}$ and $\mathfrak{a}$ motions vary as a function of shape and the frequencies of graphite are rather different from those of the finite systems. This is due to the fact that the same kind of motion varies its frequency as a consequence of confinement. In the next paragraph we will show how confinement influences vibrational frequencies in an sp^2 carbon network.

For a one-dimensional polymer it is a common procedure[25] to find relationships between short and long chains and to lay the vibrational frequencies of the short chain (oligomers) on the dispersion curves of the polymer (considered as a one-dimensional crystal). In this way a relationship is obtained between phonons of the ideally infinite polymer and normal modes of the finite molecules. This concept has also been used in order to obtain experimental phonon dispersion curves of polymers from the vibrational frequencies of short chains.[24,29]

We tried to extend such a procedure to identify phonons of graphite that reproduce both $\mathcal{H}$ and $\mathfrak{a}$ motions of the oligomers. Let us first consider the molecule of coronene. It is possible to pave the graphite lattice with coronene-shaped tiles (Fig. 10). A phonon of graphite, in order to be superimposable to a normal mode of coronene, must have nodal planes along the border between two tiles (dashed lines of Fig. 10).

The centers of the tiles form a new lattice (which we will call ''superlattice''). In order to have nodal planes along the borders of the tiles, a graphite phonon must be a $\mathbf{q}_s=\mathbf{0}$ phonon of the superlattice ($\mathbf{q}_s$ is a vector in the reciprocal lattice of the superlattice). Practically we superimpose the reciprocal lattices of graphite and of the coronene-based superlattice and we choose all the points that correspond to $\mathbf{q}_s=\mathbf{0}$ phonons of the superlattice, excluding the Γ point.

Using this method we have found the phonons of graphite that correspond to $\mathcal{H}$ and $\mathfrak{a}$ vibrations of coronene. An analogous procedure has been applied to a graphite layer paved with circumcoronene-shaped domains [see Fig. 7(c)]. We are forced to use circumcoronene instead of hexabenzocoronene because the shape of HBC is not compatible with the graphite lattice (i.e., it is not possible to pave graphite with HBC tiles).

The coordinates of the wave vectors of these phonons in the reciprocal space are

TABLE VI. Raman spectrum of HBC: vibrational assignments and calculated ideal motions contents for A_{1g} modes.

Sym. spec.	Calc. freq. (cm^{-1})	Obs. freq. (cm^{-1})	% of K vibration	Weighted content of K vibration	% of M vibration	Weighted content of M vibration
A_{1g}	3058		4	0.0410	1	0.0162
	3056		0	0.0036	3	0.0331
	1582		7	0.0692	18	0.1830
	1416		5	0.0416	36	0.2966
	1362	1312/1300	37	0.2917	25	0.1926
	1282	1263	43	0.3393	12	0.0936
	1066		7	0.0511	3	0.0212
	993		13	0.0747	13	0.0753
	723		1	0.0079	6	0.0340
	339		1	0.0011	0	0.0007

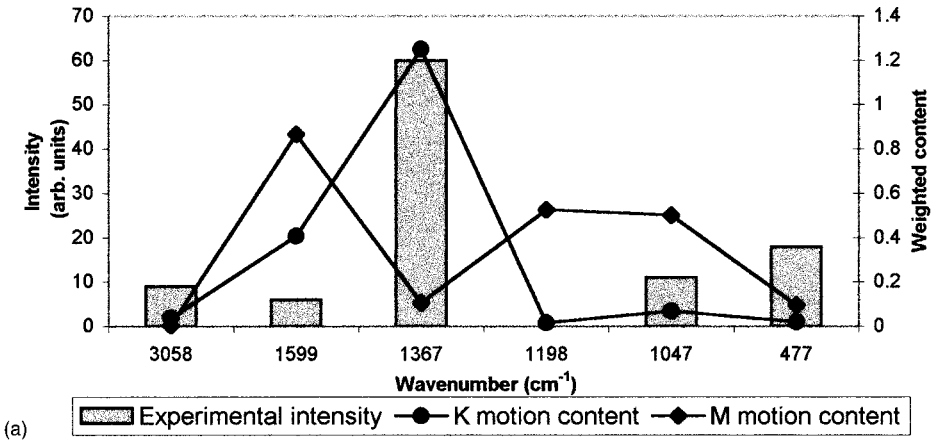

(a)

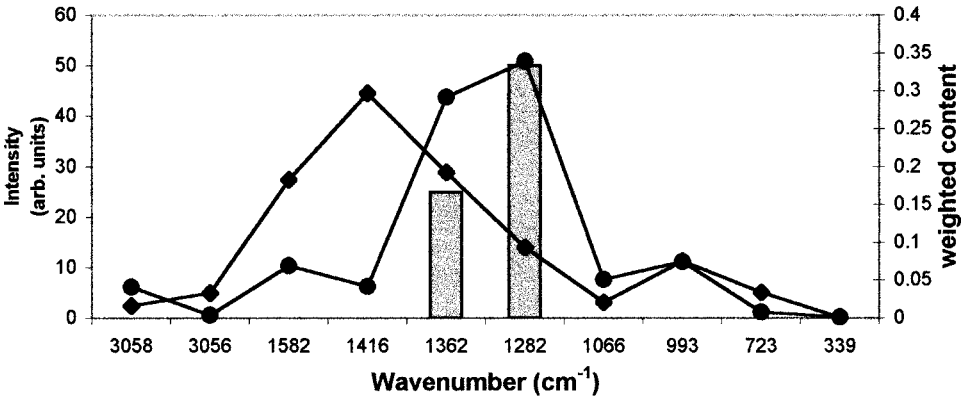

(b)

FIG. 9. Content of K and M motion in the eigenvectors of (a) coronene and (b) HBC.

Molecule	Я motion	↺ motion
Coronene	$a \equiv \left(\frac{\pi}{3}, \frac{\pi}{6}\right)$	$b \equiv \left(\frac{5}{3}\pi, \frac{5}{6}\pi\right)$
HBC	$c \equiv \left(\frac{2}{9}\pi, \frac{\pi}{9}\right)$	$d \equiv \left(\frac{14}{9}\pi, \frac{7}{9}\pi\right)$

The shapes of these phonons are shown in Fig. 11. Comparing these figures with Fig. 8 we notice that the motion of the domain is a faithful reproduction of the normal mode of the oligomer and the frequency is also close to the one calculated for the oligomer. Figure 4 shows the position of points a, b, c, and d on the dispersion curves of graphite.

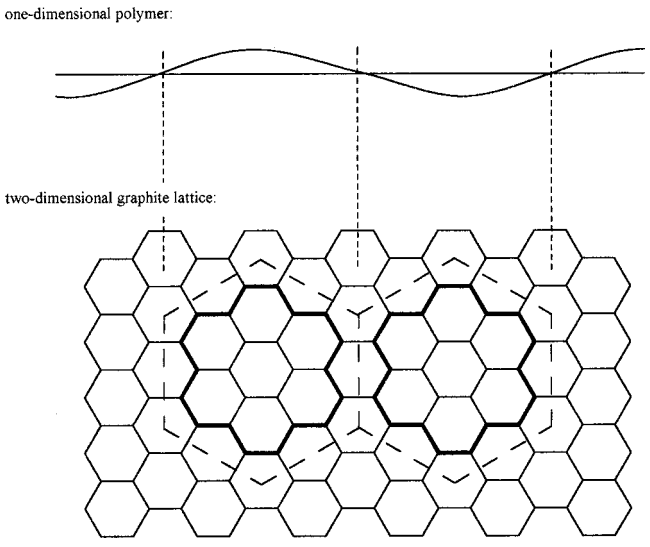

FIG. 10. Graphite paved with coronene tiles (see text).

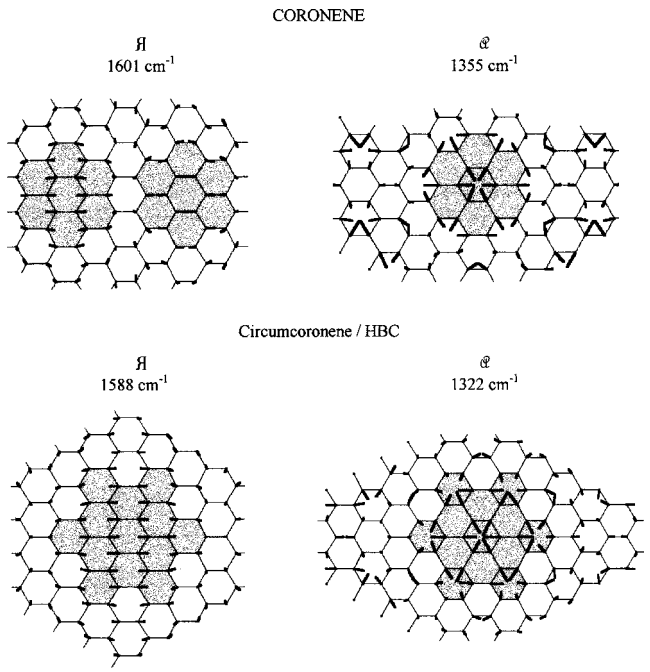

FIG. 11. Phonons of graphite that correspond to Я and ↺ motions of coronene and circumcoronene.

V. CONCLUSIONS

In the present work we have achieved the following results:

We have derived the first long-range valence force field for graphite. This field is the extension of MO/8 field, without modification of its parameters. Therefore it allows to compare the results obtained for graphite with the results given by MO/8 field on finite systems.

We present the complete treatment of in-plane vibrations in terms of valence symmetry coordinates for a single layer of graphite at the high-symmetry points of the first Brillouin zone. This treatment allows to describe, in an analytical and univocal way, the shape of the phonons of graphite at Γ, K, and M, independently of the force field used.

On the basis of such results we have done the following:

We have identified two kinds of motion of carbon sp^2 aromatic systems which produce strong Raman lines: the $\mathcal{R}$ motion and the $\mathfrak{a}$ motion. The $\mathcal{R}$ motion of a carbon sp^2 network can be described as motion where all horizontal bonds stretch in phase, while the other bonds shrink (this motion is perfectly equivalent to the other two motions obtained by rotation of the lattice of $2\pi/3$). The $\mathfrak{a}$ motion is a more complex motion which can be roughly described as a breathing mode.

We have established a correlation between these motions and two phonons of graphite: the $\mathcal{R}$ motion of oligomers, in the infinite case becomes the E_{2g} motion at Γ of graphite; the $\mathfrak{a}$ motion, in the infinite case becomes the A_1' motion of graphite at K.

We have extended to the infinite two-dimensional case a method which is usually applied to one-dimensional systems (polymers); in this way we have shown that it is possible to choose proper phonons of the infinite system which reproduce motions of small domains (oligomers).

On the basis of this analysis we can state that the D line in the Raman spectra of defected graphite samples or carbon materials can be ascribed to an $\mathfrak{a}$ motion of domains of finite size.[5] This concept will be more extensively investigated in paper which will follow shortly.[30]

ACKNOWLEDGMENTS

We thank Dr. Cremonesi of C.I.L.E.A. for his precious help with the numeric methods needed to solve the bond-bond polarizabilities integrals. This work has been partly supported by ''Progetti Finalizzati'' of the National Research Council of Italy.

[1] See, for instance, M. S. Dresselhaus and G. Dresselhaus, in *Encyclopedia of Applied Physics*, edited by G. L. Trigg, E. S. Vera, and W. Greulich (VHC, New York, 1993), Vol. 7, p. 289; M. S. Dresselhaus, G. Dresselhaus, and P. C. Eklund, *Science of Fullerenes and Carbon Nanotubes* (Academic, San Diego, 1996); J. Robertson, Adv. Phys. **35**, 317 (1986), and references quoted therein. R. J. Nemanich and S. A. Solin, Phys. Rev. B **20**, 392 (1979); P. Lespade, R. Al-Jishi, and M. S. Dresselhaus, Carbon **20**, 427 (1982); R. O. Dillon, J. A. Woollam, and V. Katkanant, Phys. Rev. B **29**, 3482 (1984); D. S. Knight and W. B. White, J. Mater. Res. **4**, 385 (1989).

[2] R. Vidano, D. B. Fishbach, L. J. Willis, and T. M. Loher, Solid State Commun. **39**, 341 (1981).

[3] M. J. Matthews, M. A. Pimenta, G. Dresselhaus, M. S. Dresselhaus, and M. Endo, Phys. Rev. B **59**, 6585 (1999).

[4] I. Póksic, M. Hunfhausen, M. Koós, and L. Ley, J. Non-Cryst. Solids **227-230**, 1083 (1998).

[5] C. Mapelli, C. Castiglioni, E. Meroni, and G. Zerbi, J. Mol. Struct. **480-481**, 615 (1999).

[6] K. Ohno, J. Mol. Spectrosc. **72**, 238 (1978); J. Chem. Phys. **95**, 5524 (1991).

[7] C. A. Coulson and H. C. Longuet-Higgins, Proc. R. Soc. London, Ser. A **193**, 447 (1948).

[8] The same formalism has been introduced by Warshel *et al.* for the calculation of potential surfaces of organic systems with conjugated π electrons. See A. Warshel and M. Karplus, J. Chem. Soc. **94**, 5612 (1972).

[9] C. A. Coulson and H. C. Longuet-Higgins, Proc. R. Soc. London, Ser. A **191**, 39 (1947).

[10] A similar treatment has been used to develop a force field for polyacetylene in L. Piseri and R. Tubino, Solid State Commun. **44**, 1589 (1982).

[11] C. A. Coulson, B. O'Leary, and R. B. Mallion, *Hückel Theory for Organic Chemists* (Academic, New York, 1978).

[12] T. Kakitani, Prog. Theor. Phys. **51**, 656 (1974).

[13] See, e.g., J. R. Scherer, J. Chem. Phys. **36**, 3308 (1962); G. Zerbi, B. Crawford, and J. Overend, *ibid.* **38**, 127 (1963); G. Zerbi and S. Sandroni, Spectrochim. Acta A **24**, 483 (1968).

[14] E. B. Wilson, Jr., J. C. Decius, and P. C. Cross, *Molecular Vibrations* (McGraw-Hill, New York, 1955).

[15] S. Califano, *Vibrational States* (Wiley, London, 1976).

[16] In the following treatment we report the analytic expressions of symmetry coordinates relative to the fundamental cell (0,0) of the lattice; the symmetry coordinate of the crystal S_{crystal} can be obtained straightforwardly by $S_{\text{crystal}}=\Sigma_{n_1 n_2} S_{(0,0)} e^{ik\cdot r}$, where $S_{(0,0)}$ is the symmetry coordinate in the fundamental cell.

[17] C. Mapelli, C. Castiglioni, and G. Zerbi, Chem. Phys. Lett. (to be published).

[18] C. Oshima, T. Aizawa, R. Souda, Y. Ishizawa, and Y. Sumiyoshi, Solid State Commun. **65**, 1601 (1988).

[19] R. Nicklow, N. Wakabayashi, and H. G. Smith, Phys. Rev. B **5**, 4951 (1972).

[20] R. J. Nemanich and S. A. Solin, Solid State Commun. **23**, 417 (1997).

[21] R. Al-Jishi and G. Dresselhaus, Phys. Rev. B **26**, 4514 (1982).

[22] R. A. Jishi, L. Venkataraman, M. S. Dresselhaus, and G. Dresselhaus, Chem. Phys. Lett. **209**, 77 (1993).

[23] G. Kresse, J. Furthmüller, and J. Hafner, Europhys. Lett. **32**, 729 (1995).

[24] M. Gussoni, C. Castiglioni, and G. Zerbi, in *Advances in Spectroscopy*, edited by R. J. H. Clark and R. E. Hester (Wiley, New York, 1991), Vol. 19, §6; G. Zerbi, M. Gussoni, and C. Castiglioni, in *Conjugated Polymers*, edited by J. L. Bredás and R. Silbey (Kluwer, Dordrecht, 1991), p. 435.

[25] R. Zbinden, *Infrared Spectroscopy of High Polymers* (Academic,

New York, 1964); P. C. Painter, M. M. Coleman, and J. L. Koenig, *The Theory of Vibrational Spectroscopy and its Application to Polymeric Materials* (Wiley, New York, 1982); G. Zerbi, Appl. Spectrosc. Rev. **2**, 193 (1969).

[26] (a) Corinna Mapelli, Ph.D. thesis, Politecnico di Milano, 1998; (b) Elvira Meroni, thesis, Advanced School in Polymer Science, Politecnico di Milano, 1999. (c) E. Meroni, G. Zerbi, and K. Müllen (unpublished).

[27] K. Yoshizawa, K. Okahara, T. Sato, K. Tanaka, and T. Yamabe, Carbon **32**, 1517 (1994).

[28] A. Stabel, P. Herwig, K. Müllen, and J. P. Raabe, Angew. Chem. Int. Ed. Engl. **34**, 1609 (1995); M. Müller, H. Mauermann-Düll, M. Wagner, V. Enkelmann, and K. Müllen, *ibid.* **34**, 1583 (1995); M. Müller, J. Petersen, R. Strohmaier, C. Günther, N. Karl, and K. Müllen, *ibid.* **35**, 886 (1996).

[29] R. J. Snyder and J. H. Schachtschneider, Spectrochim. Acta **19**, 117 (1963).

[30] C. Mapelli, C. Castiglioni, and G. Zerbi (unpublished).